

Catalysis Science & Technology

Accepted Manuscript



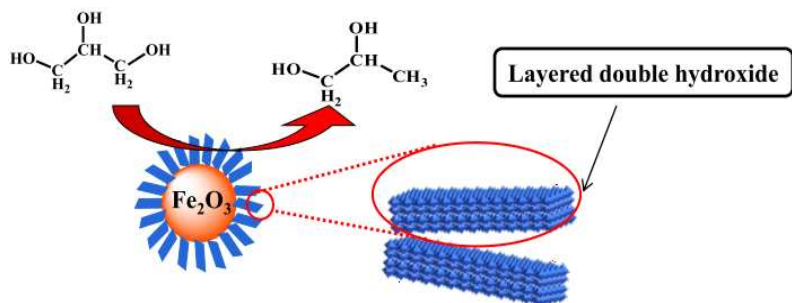
This is an *Accepted Manuscript*, which has been through the Royal Society of Chemistry peer review process and has been accepted for publication.

Accepted Manuscripts are published online shortly after acceptance, before technical editing, formatting and proof reading. Using this free service, authors can make their results available to the community, in citable form, before we publish the edited article. We will replace this *Accepted Manuscript* with the edited and formatted *Advance Article* as soon as it is available.

You can find more information about *Accepted Manuscripts* in the [Information for Authors](#).

Please note that technical editing may introduce minor changes to the text and/or graphics, which may alter content. The journal's standard [Terms & Conditions](#) and the [Ethical guidelines](#) still apply. In no event shall the Royal Society of Chemistry be held responsible for any errors or omissions in this *Accepted Manuscript* or any consequences arising from the use of any information it contains.

Graphical abstract:



Cite this: DOI: 10.1039/c0xx00000x

www.rsc.org/xxxxxx

ARTICLE TYPE

A thermally stable and easily recycled core-shell $\text{Fe}_2\text{O}_3@ \text{CuMgAl}$ catalyst for hydrogenolysis of glycerol

Shuixin Xia, Weichen Du, Liping Zheng, Ping Chen, Zhaoyin Hou*

Received (in XXX, XXX) Xth XXXXXXXXXX 20XX, Accepted Xth XXXXXXXXXX 20XX

DOI: 10.1039/b000000x

Core-shell structured magnetic $\text{Fe}_2\text{O}_3@ \text{CuMgAl}$ layered double hydroxide (LDH) catalysts were synthesized in a facile route and used in selective hydrogenolysis of glycerol. Characterizations disclosed that the thermal stability of LDH framework, the dispersion of Cu and its activity were enhanced simultaneously after the presence of Fe_2O_3 .

Catalysts in nanoparticles possess bigger surface area and higher utilization of surface atoms. They dispersed nearly homogeneously in reaction mixture and exhibited prominent activity in most reactions. These nanoparticles bring new challenge and insight to traditional catalysis and a lot of achievements were reported in recent years.¹⁻³ But catalysts in nanoparticles suffered from serious difficulty in thermal stability and must be protected by surfactants. The recovery and reuse of these nanoparticles are becoming obstacles from the perspective of green chemistry in order to achieve the ecological and economical sustainability.⁴

In order to solve these problems, great attentions have been paid to nanoparticles with magnetic properties for their efficient, reusable, sustainable and environmentally benign properties.^{5,6} Catalysts with magnetic properties can be easily separated by an external magnetic field, not only minimizing the consumption of auxiliary substances, energy and time used in separation, but also bringing significant benefits in economical and environmental aspects.^{4,7} Magnetic materials with magnetic core and functional shell, which integrate multiple functionalities into a single nanoparticle system, show great potential in catalysis.⁷⁻¹³

Layered double hydroxide compounds (LDHs), also known as "anionic clays", have attracted intense research interests in recent years because of their potential applications as solid-bases,¹⁴⁻¹⁶ catalyst supports and precursors.¹⁷⁻²⁰ LDH compounds consisted of two-dimensional brucite-type octahedral layered structures with alternating positively charged mixed metal hydroxide sheets and negatively charged interlayer anions along with water molecules.^{15,21,22} A lot of bifunctional catalysts with highly dispersed Cu^{17-19,23}, Co²⁴, or Ni^{25,26} on solid base (Mg-Al oxides) could be prepared from LDH compounds. And these catalysts exhibited prominent activity in hydrogenolysis of glycerol, removal of SO_2 and NO, dry reforming of methane. However, these catalysts in powder have suffered serious difficulty in separation, recovery and reuse in the hydrogenolysis of glycerol.^{17-19,23}

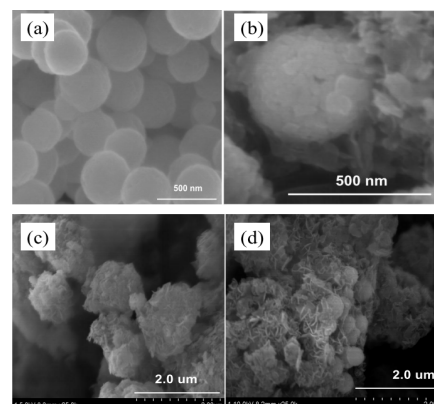


Fig. 1 SEM images of $\text{Fe}_3\text{O}_4@ \text{Cu}_{0.4}\text{Mg}_{5.6}\text{Al}_2(\text{OH})_{16}\text{CO}_3$. (a) Fe_3O_4 ; (b) (33.3%) $\text{Fe}_3\text{O}_4@ \text{Cu}_{0.4}\text{Mg}_{5.6}\text{Al}_2(\text{OH})_{16}\text{CO}_3$; (c) (16.7%) $\text{Fe}_3\text{O}_4@ \text{Cu}_{0.4}\text{Mg}_{5.6}\text{Al}_2(\text{OH})_{16}\text{CO}_3$; (d) (8.3%) $\text{Fe}_3\text{O}_4@ \text{Cu}_{0.4}\text{Mg}_{5.6}\text{Al}_2(\text{OH})_{16}\text{CO}_3$.

In this communication, an easily separated and recycled core-shell structured magnetic $\text{Fe}_2\text{O}_3@ \text{CuMgAl}$ catalyst was prepared in a facile route and used in the selective hydrogenolysis of glycerol. Fig. S1 depicted the XRD pattern of fresh $\text{Fe}_3\text{O}_4@ \text{Cu}_{0.4}\text{Mg}_{5.6}\text{Al}_2(\text{OH})_{16}\text{CO}_3$ with different contents of Fe_3O_4 . All samples displayed the characteristic diffraction peaks of a well-crystallized hydrotalcite (JCPDS 35-0965). Peaks at 11.7, 23.6, 35.0, 39.7, 47.1, 60.9 and 62.4° were assigned to the (003), (006), (012), (015), (018), (110) and (113) diffractions of LDH. However, the intensity of (003) reflection decreased with the presence of Fe_3O_4 , which suggested lower crystallinity and/or reduced particle size according to Scherrer's equation. The reflection peaks at 18.3, 30.1, 35.5 and 43.1° were assigned to characteristic diffractions of (111), (220), (311) and (400) planes of Fe_3O_4 (JCPDS 65-3107), and they enhanced with the increasing content of Fe_3O_4 .

SEM images of $\text{Fe}_3\text{O}_4@ \text{Cu}_{0.4}\text{Mg}_{5.6}\text{Al}_2(\text{OH})_{16}\text{CO}_3$ are shown in Fig. 1. It can be found that Fe_3O_4 nanosphere showed a smooth surface with a mean diameter of 300 nm (see Fig. 1-a). After coating with LDH shell, the outline of (x%) $\text{Fe}_3\text{O}_4@ \text{Cu}_{0.4}\text{Mg}_{5.6}\text{Al}_2(\text{OH})_{16}\text{CO}_3$ became rougher than that of Fe_3O_4 nanospheres, which indicated that Fe_3O_4 nanoparticles were successfully coated with the lamellae of $\text{Cu}_{0.4}\text{Mg}_{5.6}\text{Al}_2(\text{OH})_{16}\text{CO}_3$. And the thin shell of LDH lamellae

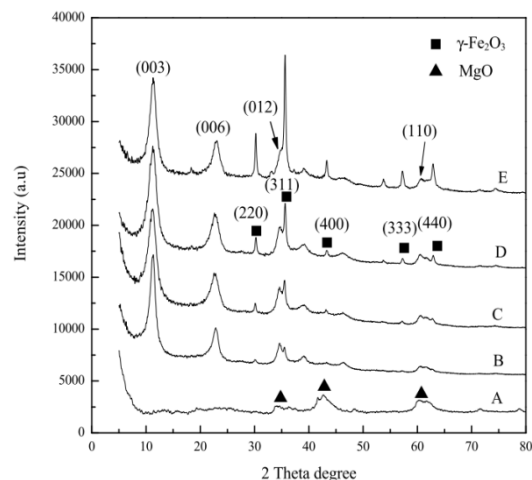


Fig. 2 XRD patterns of catalysts calcined at 400 °C. (A) pure $\text{Cu}_{0.4}\text{Mg}_{5.6}\text{Al}_2\text{O}_9$; (B) (4.2%) Fe_2O_3 @ $\text{Cu}_{0.4}\text{Mg}_{5.6}\text{Al}_2\text{O}_9$; (C) (8.3%) Fe_2O_3 @ $\text{Cu}_{0.4}\text{Mg}_{5.6}\text{Al}_2\text{O}_9$; (D) (16.7%) Fe_2O_3 @ $\text{Cu}_{0.4}\text{Mg}_{5.6}\text{Al}_2\text{O}_9$; (E) (33.3%) Fe_2O_3 @ $\text{Cu}_{0.4}\text{Mg}_{5.6}\text{Al}_2\text{O}_9$.

that coated on the surface of Fe_3O_4 nanospheres could be identified clearly in (33.3%) Fe_3O_4 @ $\text{Cu}_{0.4}\text{Mg}_{5.6}\text{Al}_2(\text{OH})_{16}\text{CO}_3$ (Fig. 1-b). The thickness of LDH lamella in shell increased with the content of LDH (see Fig. 1-c and d).

Fig. 2 shows the XRD pattern of calcined Fe_3O_4 @ $\text{Cu}_{0.4}\text{Mg}_{5.6}\text{Al}_2\text{O}_9$. It was found that the characteristic diffraction peaks of LDH disappeared completely when naked $\text{Cu}_{0.4}\text{Mg}_{5.6}\text{Al}_2(\text{OH})_{16}\text{CO}_3$ was calcined at 400 °C, 4 h (see curve A in Fig. 2), and separated MgO (JCPDS 65-0476) formed. These results meant that the lamellae structure collapsed and transformed into metal oxides after calcination at 400 °C. However, it is quite interesting to find that the characteristic diffraction peaks of LDH still remained in those samples containing iron oxide after calcination, which inferred that the thermal stability of the LDH lamellae in Fe_3O_4 @ $\text{Cu}_{0.4}\text{Mg}_{5.6}\text{Al}_2(\text{OH})_{16}\text{CO}_3$ was improved with the presence of iron oxide. At the same time, it was found that Fe_3O_4 was oxidized into $\gamma\text{-Fe}_2\text{O}_3$ during calcination. For this reason, the calcined catalyst was denoted as (x%) Fe_2O_3 @ $\text{Cu}_{0.4}\text{Mg}_{5.6}\text{Al}_2\text{O}_9$.

The improved thermal stability of LDH lamellae in Fe_3O_4 @ $\text{Cu}_{0.4}\text{Mg}_{5.6}\text{Al}_2(\text{OH})_{16}\text{CO}_3$ was also confirmed in compared XRD analysis of naked $\text{Cu}_{0.4}\text{Mg}_{5.6}\text{Al}_2(\text{OH})_{16}\text{CO}_3$ and (16.7%) Fe_3O_4 @ $\text{Cu}_{0.4}\text{Mg}_{5.6}\text{Al}_2(\text{OH})_{16}\text{CO}_3$ that calcined at different temperatures (see Fig. S2). Obvious (003) diffraction peak and slight (006) diffraction peak of LDH framework could be identified clearly in (16.7%) Fe_2O_3 @ $\text{Cu}_{0.4}\text{Mg}_{5.6}\text{Al}_2\text{O}_9$ even after calcination at 600 °C (see Fig S2-b).

TG analysis indicated that $\text{Cu}_{0.4}\text{Mg}_{5.6}\text{Al}_2(\text{OH})_{16}\text{CO}_3$ showed three major weight loss at 171, 310 and 360 °C, which could be attributed to the loss of water and carbonate.²⁷ While the corresponding weight loss in the TG profile of (16.7%) Fe_3O_4 @ $\text{Cu}_{0.4}\text{Mg}_{5.6}\text{Al}_2(\text{OH})_{16}\text{CO}_3$ located at around 219, 306 and 392 °C, respectively (see Fig. S3). An obvious phase transition peak was detected at 502.97 °C in the DSC curve of $\text{Cu}_{0.4}\text{Mg}_{5.6}\text{Al}_2(\text{OH})_{16}\text{CO}_3$,²⁸⁻³⁰ while only a faint peak appeared in (16.7%) Fe_3O_4 @ $\text{Cu}_{0.4}\text{Mg}_{5.6}\text{Al}_2(\text{OH})_{16}\text{CO}_3$ at 572.98 °C. These facts further indicated that the stability of

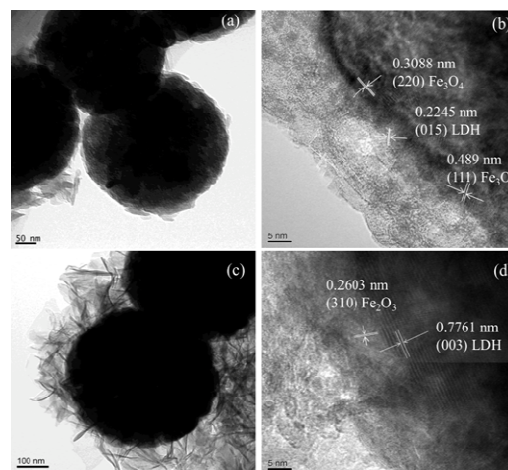


Fig. 3 TEM images of fresh (16.7%) Fe_3O_4 @ $\text{Cu}_{0.4}\text{Mg}_{5.6}\text{Al}_2(\text{OH})_{16}\text{CO}_3$ (a-b) and reduced (16.7%) Fe_2O_3 @ $\text{Cu}_{0.4}\text{Mg}_{5.6}\text{Al}_2\text{O}_9$ (c-d).

LDH framework in Fe_3O_4 @ CuMgAl LDH enhanced owing to the presence of Fe_3O_4 .

The surface composition of (x%) Fe_2O_3 @ $\text{Cu}_{0.4}\text{Mg}_{5.6}\text{Al}_2\text{O}_9$ detected in XPS was summarized in Table S1. The highest relative Cu atomic percentage of 5.8% was detected in (16.7%) Fe_2O_3 @ $\text{Cu}_{0.4}\text{Mg}_{5.6}\text{Al}_2\text{O}_9$, which is higher than the calculated Cu atomic percentage (2.1% in bulk). Thus, it could be concluded that Cu is enriched on the surface of catalysts.

This surface enrichment was also confirmed by the H_2 -TPR analysis (Fig. S4) and increased copper dispersion detected by N_2O oxidation and following H_2 titration (summarized in Table S2). Only one broader peak from 250 to 340 °C was detected in $\text{Cu}_{0.4}\text{Mg}_{5.6}\text{Al}_2\text{O}_9$, while a shoulder peak at around 160-210 °C appeared in (8.3%) Fe_2O_3 @ $\text{Cu}_{0.4}\text{Mg}_{5.6}\text{Al}_2\text{O}_{8.6}$, and this peak enhanced with increasing the content of Fe_2O_3 . The dispersion of copper in $\text{Cu}_{0.4}\text{Mg}_{5.6}\text{Al}_2\text{O}_{8.6}$ was only 43.2%, however, this value increased to 62.8% in (8.3%) Fe_2O_3 @ $\text{Cu}_{0.4}\text{Mg}_{5.6}\text{Al}_2\text{O}_{8.6}$. That is, the dispersion of copper was improved with the presence of iron oxide.

Nitrogen adsorption-desorption isotherms of reduced (x%) Fe_2O_3 @ $\text{Cu}_{0.4}\text{Mg}_{5.6}\text{Al}_2\text{O}_{8.6}$ are shown in Fig. S5(a). All of them are type IV pattern according to the International Union of Pure and Applied Chemistry (IUPAC) classification. The closure point of hysteresis loop of $\text{Cu}_{0.4}\text{Mg}_{5.6}\text{Al}_2\text{O}_{8.6}$ located at a relative pressure of 0.5, however, with the incorporation of Fe_2O_3 , the closure point of hysteresis loop shifted to 0.8, which indicated that the pore diameter increased with the presence of Fe_2O_3 . The calculated surface area of naked $\text{Cu}_{0.4}\text{Mg}_{5.6}\text{Al}_2\text{O}_{8.6}$ was 127.9 m^2/g , and it is interesting to note that the surface area of (4.2%) Fe_2O_3 @ $\text{Cu}_{0.4}\text{Mg}_{5.6}\text{Al}_2\text{O}_{8.6}$ and (8.3%) Fe_2O_3 @ $\text{Cu}_{0.4}\text{Mg}_{5.6}\text{Al}_2\text{O}_{8.6}$ increased to 144.5 and 141.7 m^2/g , respectively (see Table S2). The increased surface area might be attributed to the reduced size of solid lamellae and the ordered arrangement of these lamellae on the surface of Fe_2O_3 core (see Fig. S1).

The pore size distribution of reduced (x%) Fe_2O_3 @ $\text{Cu}_{0.4}\text{Mg}_{5.6}\text{Al}_2\text{O}_{8.6}$ was calculated and presented in Fig. S5(b). Only one peak (at around 1.8-4.4 nm) was

Cite this: DOI: 10.1039/c0xx00000x

www.rsc.org/xxxxxx

ARTICLE TYPE

Table 1 Glycerol hydrogenolysis over different catalysts ^a.

Catalysts	Conversion (%)	Activity of surface Cu (h ⁻¹) ^b	Selectivity (%)	
			1,2-PDO	Others ^c
Cu _{0.4} /Mg _{5.6} Al ₂ O _{8.6}	18.6	5.5	98.6	1.4
(4.2%)Fe ₂ O ₃ @Cu _{0.4} /Mg _{5.6} Al ₂ O _{8.6}	72.1	15.9	99.1	0.9
(8.3%)Fe ₂ O ₃ @Cu _{0.4} /Mg _{5.6} Al ₂ O _{8.6}	77.8	15.8	99.0	1.0
(16.7%)Fe ₂ O ₃ @Cu _{0.4} /Mg _{5.6} Al ₂ O _{8.6}	76.2	16.5	99.3	0.7
(33.3%)Fe ₂ O ₃ @Cu _{0.4} /Mg _{5.6} Al ₂ O _{8.6}	49.1	11.2	98.8	1.2

^a Reaction conditions: 10.9 mmol glycerol in ethanol solution (413 mmol), and 0.085 mmol Cu, 2.0 MPa H₂, 190 °C, 10 h. ^b Defined as (mol of converted glycerol)/(mol of exposed Cu atom)/(reaction time, h). ^c Ethylene glycol, methanol and 1-propanol.

detected in Cu_{0.4}/Mg_{5.6}Al₂O_{8.6}, which could be attributed to the accumulation of LDH lamellae in reduced Cu_{0.4}/Mg_{5.6}Al₂O_{8.6}. With the presence of iron oxides, another mesopore at around 44 nm could be observed, and this mesopore channel could be ascribed to the gap of vertical arranged LDH lamellae on the surface of Fe₂O₃ (see Fig. 3-c). TEM images of (16.7%)Fe₃O₄@Cu_{0.4}/Mg_{5.6}Al₂(OH)₁₆CO₃ and reduced (16.7%)Fe₂O₃@Cu_{0.4}/Mg_{5.6}Al₂O_{8.6} were shown in Fig. 3. It can be found that thin LDH shell was coated on the surface of Fe₃O₄ in (16.7%)Fe₃O₄@Cu_{0.4}/Mg_{5.6}Al₂(OH)₁₆CO₃ LDH shell could be identified clearly in HRTEM image (Fig. 3(b)). Ordered lattice fringes at 0.3088 and 0.489 nm could be indexed to the (220) and (111) planes of the Fe₃O₄ phase. Lattice fringe at 0.2245 nm in the margin area was designated to the (015) plane of Cu_{0.4}/Mg_{5.6}Al₂(OH)₁₆CO₃ LDH phase. The three-dimensional core-shell architecture of reduced (16.7%)Fe₂O₃@Cu_{0.4}/Mg_{5.6}Al₂O_{8.6} displayed a flowerlike morphology (see Fig. 3(c)), most petal-like LDH nanoplatelets are perpendicularly coated on the surface of the solid core. Under higher resolution, ordered lattice fringes at 0.2603 and 0.7761 nm could be detected, which corresponded to the (310) plane of γ-Fe₂O₃ and the (003) plane of LDH.

The basicity of the catalyst was characterized via the CO₂ adsorption by TG-DSC and the results were summarized in Table S3. It was found that with the presence of Fe₂O₃, the amount of adsorbed CO₂ increased, which meant the basicity of the catalyst enhanced with the presence of Fe₂O₃. The enhanced basicity could be ascribed to the increased surface area and pore volume of the catalysts brought in by the incorporation of iron oxide (see Table S2).

Glycerol is a poly-functionalized platform chemical derived from bio-sustainable resources.³¹ Hydrogenolysis of glycerol to propanediols (PDOs) is one of the most promising and vital transformations of the oversupplied glycerol in order to achieve the sustainable development of biodiesel industry.^{18,19,32-51} In our previous work, we found that CuMgAl LDH were efficient catalysts for this process.^{17-19,23} However, separation of powder catalysts from reaction mixture is difficult and time-/energy-consuming. In order to achieve the easy separation of catalyst and product, the magnetic catalyst would be a good choice. The above

synthesized magnetic Fe₂O₃@Cu_{0.4}/Mg_{5.6}Al₂O_{8.6} catalysts were investigated in the glycerol hydrogenolysis reactions.

Table 1 summarized the activity of (x%)Fe₂O₃@Cu_{0.4}/Mg_{5.6}Al₂O_{8.6} for hydrogenolysis of glycerol at 190 °C in ethanol solvent. The conversion of glycerol was only 18.6% over naked Cu_{0.4}/Mg_{5.6}Al₂O_{8.6} and the calculated activity of surface Cu atom was 5.5 h⁻¹. It can be found that the activity of surface Cu atom increased obviously with the presence of Fe₂O₃. The conversion of glycerol reached 77.8 and 76.2% over (8.3%)Fe₂O₃@Cu_{0.4}/Mg_{5.6}Al₂O_{8.6} and (16.7%)Fe₂O₃@Cu_{0.4}/Mg_{5.6}Al₂O_{8.6}, respectively. The TOF of surface Cu in (16.7%)Fe₂O₃@Cu_{0.4}/Mg_{5.6}Al₂O_{8.6} reached 16.5 h⁻¹, and this value is higher than that of our previous reported Rh_{0.02}Cu_{0.4}/Mg_{5.6}Al_{1.98}O_{8.57},¹⁷ Pd_{0.04}Cu_{0.4}/Mg_{5.56}Al₂O_{8.56},¹⁸ and Cu_{0.4}/Zn_{0.6}Mg_{5.0}Al₂O_{8.6} catalysts¹⁹ under same condition (see Table S4). In previous works, we found that the activity of surface Cu in CuMgAl catalyst depended mainly on its basicity,^{19,23,50} the increased activity of Cu in Fe₂O₃@CuMgAl could be attributed to its stronger basicity (see Table S3). At the same time, the increased surface area (see Table S2), and the newly formed mesopore at around 44 nm in Fe₂O₃@Cu_{0.4}/Mg_{5.6}Al₂O_{8.6} (see Fig. S5) would also promote the accessibility of glycerol to surface Cu and enhance its activity. (33.3%)Fe₂O₃@Cu_{0.4}/Mg_{5.6}Al₂O_{8.6} and (16.7%)Fe₂O₃@Cu_{0.4}/Mg_{5.6}Al₂O_{8.6} could be separated easily with a single external magnetic field (Fig. S6).

Fig. S7 presents the activity of recycled (16.7%)Fe₂O₃@Cu_{0.4}/Mg_{5.6}Al₂O_{8.6} catalyst. The conversion of glycerol decreased slightly from 76.2 to 68.1% in five successive usages, while the selectivity remained higher than 98.4%. The actual compositions of fresh catalyst and five-recycled catalyst were detected and compared (see Table S5). No leaching of Cu was observed after five successive recycled usages. These results inferred that this catalyst was stable for the selective hydrogenolysis of glycerol.

In summary, a series of functionalized core-shell structured magnetic Fe₂O₃@CuMgAl LDH catalysts could be fabricated by a facile route. The thermal stability of LDH, the dispersion of Cu in Fe₂O₃@CuMgAl LDH catalysts enhanced owing to the presence of Fe₂O₃. These catalysts are effective for their higher activity, easiness in separation in the selective hydrogenolysis of glycerol.

Notes and references

Key Lab of Applied Chemistry of Zhejiang Province, Department of Chemistry, Zhejiang University, Hangzhou 310028, China. Fax: +86-571-88273283; Tel: +86-571-88273272; E-mail: zyhou@zju.edu.cn

† Electronic Supplementary Information (ESI) available: [details of any supplementary information available should be included here]. See DOI: 10.1039/b000000x/

‡ This work was supported by National Natural Science Foundation of China (21273198, 21073159) and Zhejiang Provincial Natural Science Foundation (LZ12B03001).

- 1 A. Wittstock, V. Zielasek, J. Biener, C. M. Friend and M. Bäumer, *Science*, 2010, **327**, 319.
- 2 A. Corma, P. Concepción, M. Boronat, M. J. Sabater, J. Navas, M. J. Yacaman, E. Larios, A. Posadas, M. A. López-Quintela, D. Buceta, E. Mendoza, G. Guilera and A. Mayoral, *Nat. Chem.*, 2013, **5**, 775.
- 3 S. Guo and S. Sun, *J. Am. Chem. Soc.*, 2012, **134**, 2492.
- 4 S. Shylesh, V. Schünemann and W. R. Thiel, *Angew. Chem. Int. Ed.*, 2010, **49**, 3428.
- 5 L. Li, Y. Feng, Y. Li, W. Zhao and J. Shi, *Angew. Chem. Int. Ed.*, 2009, **48**, 5888.
- 6 K. Jiang, H.-X. Zhang, Y.-Y. Yang, R. Mothes, H. Lang and W.-B. Cai, *Chem. Commun.*, 2011, **47**, 11924.
- 7 L. Guo, J. Zhou, J. Mao, X. Guo and S. Zhang, *Appl. Catal. A*, 2009, **367**, 93.
- 8 H. Zhang, D. Pan and X. Duan, *J. Phys. Chem. C*, 2009, **113**, 12140.
- 9 D. Pan, H. Zhang, T. Fan, J. Chen and X. Duan, *Chem. Commun.*, 2011, **47**, 908.
- 10 E. S. Vasiliadou, E. Heracleous, I. A. Vasalos and A. A. Lemonidou, *Appl. Catal. B*, 2009, **92**, 90.
- 11 F. Mi, X. Chen, Y. Ma, S. Yin, F. Yuan and H. Zhang, *Chem. Commun.*, 2011, **47**, 12804.
- 12 H. Zhang, G. Zhang, X. Bi and X. Chen, *J. Mater. Chem. A*, 2013, **1**, 5934.
- 13 A.-H. Lu, E. L. Salabas and F. Schüth, *Angew. Chem. Int. Ed.*, 2007, **46**, 1222.
- 14 G. Busca, *Chem. Rev.*, 2010, **110**, 2217.
- 15 J. S. Valente, H. Pfeiffer, E. Lima, J. Prince and J. Flores, *J. Catal.*, 2011, **279**, 196.
- 16 S. He, Z. An, M. Wei, D. G. Evans and X. Duan, *Chem. Commun.*, 2013, **49**, 5912.
- 17 S. Xia, Z. Yuan, L. Wang, P. Chen and Z. Hou, *Bioresour. Technol.*, 2012, **104**, 814.
- 18 S. Xia, Z. Yuan, L. Wang, P. Chen and Z. Hou, *Appl. Catal. A*, 2011, **403**, 173.
- 19 S. Xia, R. Nie, X. Lu, L. Wang, P. Chen and Z. Hou, *J. Catal.*, 2012, **296**, 1.
- 20 N. Barrabes, D. Cornado, K. Foettinger, A. Dafinov, J. Llorca, F. Medina and G. Rupprechter, *J. Catal.*, 2009, **263**, 239.
- 21 P. J. Sideris, U. G. Nielsen, Z. Gan and C. P. Grey, *Science*, 2008, **321**, 113.
- 22 M. Shao, M. Wei, D. G. Evans and X. Duan, *Chem. Commun.*, 2011, **47**, 3171.
- 23 Z. Yuan, L. Wang, J. Wang, S. Xia, P. Chen, Z. Hou and X. Zheng, *Appl. Catal. B*, 2011, **101**, 431.
- 24 A. E. Palomares, J. M. López-Nieto, F. J. Lázaro, A. López and A. Corma, *Appl. Catal. B*, 1999, **20**, 257.
- 25 K. Takehira, T. Shishido, P. Wang, T. Kosaka and K. Takaki, *J. Catal.*, 2004, **221**, 43.
- 26 T. Shishido, M. Sukenobu, H. Morioka, M. Kondo, Y. Wang, K. Takaki and K. Takehira, *Appl. Catal. A*, 2002, **223**, 35.
- 27 J. Zhang, Y. F. Xu, G. Qian, Z. P. Xu, C. Chen and Q. Liu, *J. Phys. Chem.*, 2010, **114**, 10768.
- 28 F. Leroux and J.-P. Besse, *Chem. Mater.*, 2001, **13**, 3507.
- 29 S. J. Roosendaal, B. van Asselen, J. W. Elsenaar, A. M. Vredenberg and F. H. P. M. Habraken, *Surf. Sci.*, 1999, **442**, 329.
- 30 T. Yamashita and P. Hayes, *Appl. Surf. Sci.*, 2008, **254**, 2441.
- 31 Z. Lin, H. Chu, Y. Shen, L. Wei, H. Liu and Y. Li, *Chem. Commun.*, 2009, 7167.
- 32 J. Oh, S. Dash and H. Lee, *Green Chem.*, 2011, **13**, 2004.
- 33 Y. Nakagawa, Y. Shinmi, S. Koso and K. Tomishige, *J. Catal.*, 2010, **272**, 191.
- 34 I. Gandarias, P. L. Arias, J. Requies, M. B. Güemez and J. L. G. Fierro, *Appl. Catal. B*, 2010, **97**, 248.
- 35 J. Zhou, J. Zhang, X. Guo, J. Mao and S. Zhang, *Green Chem.*, 2012, **14**, 156.
- 36 Y. Nakagawa and K. Tomishige, *Catal. Sci. Technol.*, 2011, **1**, 179.
- 37 Z. Wu, Y. Mao, X. Wang and M. Zhang, *Green Chem.*, 2011, **13**, 1311.
- 38 S. Xia, L. Zheng, W. Ning, L. Wang, P. Chen and Z. Hou, *J. Mater. Chem. A*, 2013, **1**, 11548.
- 39 A. Bienholz, F. Schwab and P. Claus, *Green Chem.*, 2010, **12**, 290.
- 40 W. Yu, J. Zhao, H. Ma, H. Miao, Q. Song and J. Xu, *Appl. Catal. A*, 2010, **383**, 73.
- 41 I. Gandarias, P. L. Arias, J. Requies, M. El Doukkali and M. B. Güemez, *J. Catal.*, 2011, **282**, 237.
- 42 M. G. Musolino, L. A. Scarpino, F. Mauriello and R. Pietropaolo, *ChemSusChem*, 2011, **4**, 1143.
- 43 S. Zhu, Y. Zhu, S. Hao, H. Zheng, T. Mo and Y. Li, *Green Chem.*, 2012, **14**, 2607.
- 44 Z. Xiao, S. Jin, X. Wang, W. Li, J. Wang and C. Liang, *J. Mater. Chem.*, 2012, **22**, 16598.
- 45 Z. Xiao, C. Li, J. Xiu, X. Wang, C. T. Williams and C. Liang, *J. Mol. Catal. A: Chem.*, 2012, **365**, 24.
- 46 N. D. Kim, J. R. Park, D. S. Park, B. K. Kwak and J. Yi, *Green Chem.*, 2012, **14**, 2638.
- 47 S. Zhu, X. Gao, Y. Zhu, Y. Zhu, H. Zheng and Y. Li, *J. Catal.*, 2013, **303**, 70.
- 48 Y. Shinmi, S. Koso, T. Kubota, Y. Nakagawa and K. Tomishige, *Appl. Catal. B*, 2010, **94**, 318.
- 49 Y. Amada, Y. Shinmi, S. Koso, T. Kubota, Y. Nakagawa and K. Tomishige, *Appl. Catal. B*, 2011, **105**, 117.
- 50 Z. Yuan, J. Wang, L. Wang, W. Xie, P. Chen, Z. Hou and X. Zheng, *Bioresour. Technol.*, 2010, **101**, 7088.
- 51 Y. Nakagawa, X. Ning, Y. Amada and K. Tomishige, *Appl. Catal. A*, 2012, **433-434**, 128.